



Quantum dot-based microfluidic biosensor for cancer detection

Aditya Sharma Ghrera, Chandra Mouli Pandey, Md. Azahar Ali, and Bansi Dhar Malhotra

Citation: [Applied Physics Letters](#) **106**, 193703 (2015); doi: 10.1063/1.4921203

View online: <http://dx.doi.org/10.1063/1.4921203>

View Table of Contents: <http://scitation.aip.org/content/aip/journal/apl/106/19?ver=pdfcov>

Published by the [AIP Publishing](#)

Articles you may be interested in

[Rapid microfluidic solid-phase extraction system for hyper-methylated DNA enrichment and epigenetic analysis](#)
Biomicrofluidics **8**, 054119 (2014); 10.1063/1.4899059

[Planar lens integrated capillary action microfluidic immunoassay device for the optical detection of troponin I](#)
Biomicrofluidics **7**, 064112 (2013); 10.1063/1.4837755

[On-chip microfluidic biosensor using superparamagnetic microparticles](#)
Biomicrofluidics **7**, 054117 (2013); 10.1063/1.4826546

[Solid-state sensor incorporated in microfluidic chip and magnetic-bead enzyme immobilization approach for creatinine and glucose detection in serum](#)
Appl. Phys. Lett. **99**, 253704 (2011); 10.1063/1.3671078

[Electrical detection of proteins and DNA using bioactivated microfluidic channels: Theoretical and experimental considerations](#)
J. Vac. Sci. Technol. B **27**, 3099 (2009); 10.1116/1.3264675

AIP | APL Photonics

APL Photonics is pleased to announce
Benjamin Eggleton as its Editor-in-Chief



Quantum dot-based microfluidic biosensor for cancer detection

Aditya Sharma Ghrera,^{1,2} Chandra Mouli Pandey,¹ Md. Azahar Ali,¹
 and Bansi Dhar Malhotra^{3,a)}

¹Biomedical Instrumentation Section, CSIR-National Physical Laboratory, New Delhi-110012, India

²School of Engineering and Technology, ITM University, Gurgaon-122017, India

³Department of Biotechnology, Delhi Technological University, Delhi-110042, India

(Received 25 February 2015; accepted 5 May 2015; published online 15 May 2015)

We report results of the studies relating to fabrication of an impedimetric microfluidic-based nucleic acid sensor for quantification of DNA sequences specific to chronic myelogenous leukemia (CML). The sensor chip is prepared by patterning an indium–tin–oxide (ITO) coated glass substrate via wet chemical etching method followed by sealing with polydimethylsiloxane (PDMS) microchannel for fluid control. The fabricated microfluidic chip comprising of a patterned ITO substrate is modified by depositing cadmium selenide quantum dots (QCdSe) via Langmuir–Blodgett technique. Further, the QCdSe surface has been functionalized with specific DNA probe for CML detection. The probe DNA functionalized QCdSe integrated miniaturized system has been used to monitor target complementary DNA concentration by measuring the interfacial charge transfer resistance via hybridization. The presence of complementary DNA in buffer solution significantly results in decreased electroconductivity of the interface due to presence of a charge barrier for transport of the redox probe ions. The microfluidic DNA biosensor exhibits improved linearity in the concentration range of 10^{-15} M to 10^{-11} M. © 2015 AIP Publishing LLC. [<http://dx.doi.org/10.1063/1.4921203>]

The microfluidic based biosensors are being extensively explored for point-of-care (POC) diagnostic applications since they offer many advantages in terms of reagent consumption, multiplexing, parallelization, less biorecognition time, portability, and design versatility.^{1,2} Several characteristics of small scale fluid flow in microfluidics, including laminar flow, and easy fluid control can be achieved via micro-scale fluid regulators such as micropump or valve.^{2,3} The miniaturization of numerous bioassays via lab-on-a-chip (LOC) format can be used to investigate polymerase chain reaction, DNA and cellular analysis, DNA sequencing, immunoassays, and electrophoresis.^{4,5}

The development of electrochemical biosensors for clinical diagnostics has recently aroused much interest due to their high sensitivity, capability of precise target recognition, and efficient signal transduction.^{6,7} Electrochemical transduction of DNA hybridization relies on monitoring the change in surface properties such as capacitance and impedance with the help of a redox-active species.² In case of the DNA hybridization process, wherein the biosensor chip having probe DNA is immersed into a target DNA solution, the diffusion of target DNA to the probe DNA limits the hybridization efficiency.⁸ To overcome this problem, electrochemical DNA biosensors can be integrated with microfluidic to accomplish active diffusion of the target with immobilized probes and achieve improved sensitivity of the device.^{2,9,10} Direct electrochemical detection of DNA hybridization can be performed via electrochemical impedance spectroscopy (EIS), which monitors the increased surface charge on the chip as a result of DNA hybridization.^{11,12} In this context, a diffusion-restriction model can be applied to miniaturized EIS based biochip nano-volume reactor. This model has

been found to facilitate characterization of DNA hybridization events that contribute to both enhanced diffusion and charge transfer resistance.⁹ The functionality and the specificity of biosensor have also been tested with DNA hybridization events on both macro- and micro-biochips. Recently, Kim *et al.* have reported a DNA sensor with unique 3D micro-fluidic-channel having the probe DNA immobilized in its inner walls.¹⁰

The recent advances in nanotechnology have led to enhanced sensitivity of the devices enabling them to detect small variations in desired specimens. Different facet of the detection system based on nanomaterials in diversified forms including tagging of capture probe, chip fabrication, and chip coatings can be used to obtain higher signal intensities, improved biocompatibility, additional binding sites, etc.^{13,14} Quantum dots (QDs) are known to provide a large specific surface area and excellent surface activity thereby enhancing the charge transfer across the sensor chip/electrolyte interface.¹⁵ The optimized experimental conditions to obtain stable Langmuir monolayer and Langmuir–Blodgett (LB) deposition of CdSe quantum dots (QCdSe) film have been previously reported by our group. The film was subsequently employed for the fabrication of electrochemical DNA sensor.¹⁶

In the present work, a microfluidic biochip has been designed via wet chemical etching and soft lithographic techniques and QCdSe-LB film has been employed as the transducer surface for chronic myelogenous leukemia (CML) specific biochip fabrication. CML is a haematological disorder characterized by increased proliferation of the granulocytic cell-line without the loss of their capacity to differentiate. More than 95% of cases result from a cytogenetic aberration known as the Philadelphia chromosome arising from t(9;22) (q34;q11) reciprocal translocation. This translocation leads to generation of the BCR–ABL oncogene that code for chimeric tyrosine kinase. The normal tyrosine kinase regulates

^{a)} Author to whom correspondence should be addressed. Electronic mail: bansi.malhotra@gmail.com

proliferation and survival of normal cells; however, its hyperactivity disrupts this fine balance and leads to the production of cells that are endowed with proliferative advantages, such as blocking of apoptosis, genome instability, and suppression of normal hematopoiesis, thereby providing the pathogenesis for CML. In our previous report, the LB film of QCdSe was employed for the fabrication of electrochemical DNA sensor for CML detection.¹⁶ The integration of LB film of QCdSe with microfluidic assembly has further improved sensing performance of the CML specific biochip.

For the fabrication of the microfluidic chip, indium–tin–oxide (ITO) coated (thickness ~ 150 Å) glass substrate having sheet resistance of ~ 30 Ω has been employed. Using wet chemical etching method, ITO coating is patterned into a desired dimension ($2\text{ mm} \times 2.5\text{ cm}$) on the glass substrate.¹⁷ For etching process, the ITO ($2.5 \times 3.0\text{ cm}$) is selectively masked ($2\text{ mm} \times 2.5\text{ cm}$) at two positions (0.5 cm apart) using a masking tape followed by dipping in the etchant solution [$\text{HNO}_3\text{:HCl:H}_2\text{O}$ ($1\text{:}10\text{:}10$)] for about 15 min. The solution etches the exposed ITO layer, whereas the masked ITO is left un-etched. The obtained pattern is cleaned with acetone and washed with water. One of the electrodes on the chip is modified with QCdSe using LB deposition method to serve as the working electrode (WE) and other one is used as counter electrode (CE) (Figure 1). The WE is hydrophobized via previously reported procedure and is subjected to LB deposition of QCdSe under optimized experimental conditions.¹⁶ Briefly, a monolayer of QCdSe–SA is deposited onto WE at optimized experimental conditions (20°C , 38 mN m^{-1}). The HRTEM image shown in Figure S1 (Ref. 23) reveals the preservation of the ordered arrangement of particulates (existing at the air–water interface) even after transferring to the solid substrate (200–mesh carbon coated Cu grid).

For biochip preparation, thiol terminated DNA probe is covalently immobilized on the WE using Cd–thiol affinity. For this purpose, $40\text{ }\mu\text{l}$ of pDNA ($1.0\text{ }\mu\text{M}$) was spread onto the

surface of electrode, containing LB assembly of trioctylphosphine oxide (TOPO) capped CdSe QD, and incubated at 25°C to allow displacement of surface TOPO molecules with the –SH terminal of pDNA. To characterize the assembly of QCdSe at the single-particle level and monitor the topographic status of the biochip, atomic force microscopy (AFM) has been used. Figure 2 shows the topography and 3D AFM images of QCdSe modified electrode. As revealed by AFM imaging, the deposited QCdSe exhibit a homogeneous and symmetrical distribution over the electrode surface with an average height of the monolayer film as 3 nm (Figures 2(a) and 2(b)). The measured average height of QCdSe–LB film is smaller than the average diameter of QCdSe measured by TEM (4 nm). This may either be due to the compression effect of AFM tips or because of closed packed arrangement of particles that minimize the inter-particle gaps and thus the average height from the substrate surface. Further, modification of the QCdSe–LB monolayer film with probe DNA results in an increased average height (6.91 nm) (Figures 2(c) and 2(d)), which is consistent with the fact that DNA molecules have bigger size compared to the QCdSe used for present studies. Also, since the immobilization of DNA probe has been accomplished via self-assembly technique, the surface density of DNA molecules is dependent on various parameters including the solution concentration and the binding efficiency of DNA on QCdSe. Thus, the increased average height of the biochip may be due to agglomeration of the pDNA or incomplete formation of monolayer structure. Thus, results of the AFM studies confirm the presence of ordered assembly of QCdSe on electrode surface and also the sequential immobilization of DNA probe.

Soft lithography technique is used for the fabrication of polydimethylsiloxane (PDMS) microchannels having dimension of $200\text{ mm} \times 200\text{ mm} \times 2\text{ cm}$ (width \times height \times length). Using the photoresist spinner, the 200 mm thick coating of the negative SU-8 photoresist over a silicon wafer is performed. The wafer is heated at 100°C to evaporate the solvent and the UV radiation is passed through it using a desired photomask. It is again heated at 110°C to bring about selective cross-links in the uncovered part of SU-8. Using developer, the covered SU-8 is thereafter removed to obtain the master. Before use, the wafer is subjected to cleaning with acetone and exposure to fuming HNO_3 . Mixing of PDMS prepolymer and curing agent (Sylgard 184, Dow Corning) is done in $10\text{:}1$ ratio (v/v) followed by pouring of the degassed mixture over the master. The mixture is allowed to cure for about 30 min at 80°C and then PDMS replica is peeled off from the master. In the PDMS slab, the holes are punched at desired positions to form reservoirs. Thereafter, the slab is sealed with the patterned ITO substrate having working and counter electrodes.¹⁸ In the inlet reservoir, the syringe pump is introduced; while in the outlet reservoir of the microchannel, a silver wire (0.4 mm diameter) having Ag/AgCl coating is introduced as the reference electrode.

Miniaturization of electrochemical microfluidic (MF) devices is known to result in variation of the physical and chemical parameters. Prior to application of the QCdSe based chip for the biosensing, its electrochemical behaviour is experimentally characterized through EIS using $5\text{ mM K}_3[\text{Fe}(\text{CN})_6]^{3-/4-}$. One of the dominant effects of EIS based biosensor is the change in electrode/electrolyte interfacial

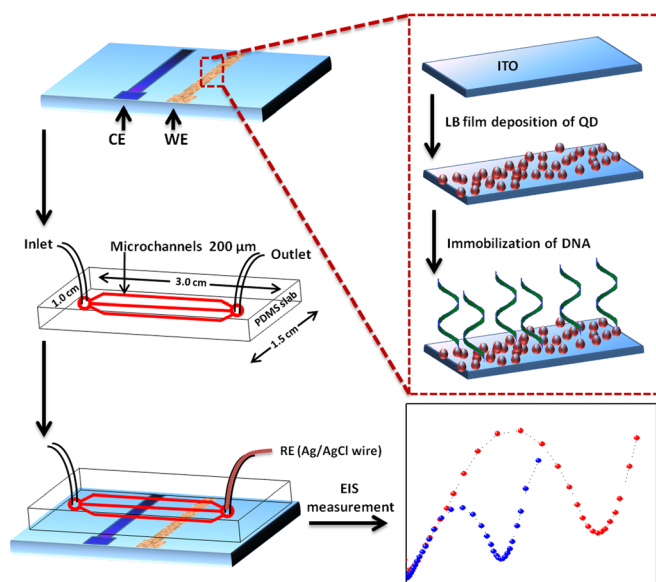


FIG. 1. Different steps showing the fabrication of microfluidic biochip for electrochemical detection of DNA hybridization. WE: Working electrode, CE: Counter electrode, and RE: Reference electrode.

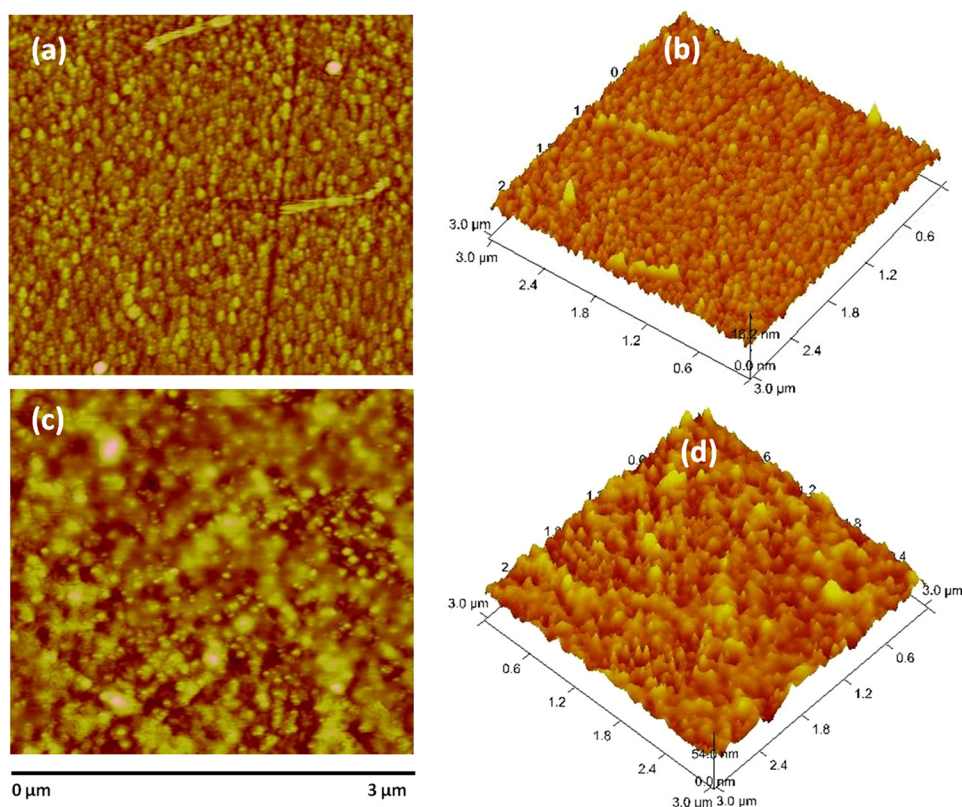


FIG. 2. 2D and 3D AFM images showing (a) and (b) LB deposition of QCdSe on working electrode of the chip, and (c) and (d) immobilization of DNA probe onto LB deposited QCdSe, respectively.

properties in response to a small AC signal as a function of frequency.^{19,20} Microfluidic devices use low sample volumes and provide fast reaction rates due to the smaller diffusion distances, and a diffusion restriction model can be applied.⁹ The bioelectrical model includes both energy storage and dissipation elements and is shown in Figure S2.²³ In the equivalent circuit, R_s is the solution resistance, R_{ct} is the charge transfer resistance at the counter electrode (R_{ct-c}), and at the working electrode (R_{ct-w}), C_{dl} is the electrode-electrolyte double layer interface at the counter electrode (C_{dl-c}) and the working electrode (C_{dl-w}), and M is the restricted linear diffusion impedance element.²¹

To understand the effect of flow rate on the biochip, EIS spectra of the biochip as a function of buffer flow rate ($0.1\text{--}1.4\ \mu\text{L min}^{-1}$) is recorded (Figure S3).²³ The R_{ct} value is found to gradually increase with respect to flow rate of the buffer solution (having $[\text{Fe}(\text{CN})_6]^{3-/4-}$ ions) that may perhaps be due to increased fluid velocity. Nevertheless, the increase in R_{ct} is observed till the flow rate of $1.0\ \mu\text{L min}^{-1}$, after which it gets saturated. At $1.0\ \mu\text{L min}^{-1}$ flow rate, the response time of the microfluidics electrode is 60 s, after which the R_{ct} value of the biochip does not significantly change.

The Faradic impedance changes as a result of biochip modification process prior to and after incubation with $10\ \mu\text{M}$ target DNA have been investigated in the frequency range of $10^5\text{--}0.1\ \text{Hz}$.¹¹ The Nyquist plot for the Faradic impedance spectrum is presented in Figure 3. In the Nyquist plot of the impedance spectra, a usual semicircle is observed which corresponds to the electron transfer resistance process (R_{ct}) and the magnitude of R_{ct} depends on the dielectric and insulating features that can be used to interpret electrode-electrolyte interface properties.²⁰ The modification over the chip surface causes a change in its R_{ct} value and in case of a

DNA biosensor, the change in R_{ct} value may be induced by hybridization or the conformational changes of DNA to an electrical signal.¹² The modification of QCdSe-LB/ITO electrode with DNA probe, results in an increased R_{ct} value of chip from $6.7\ \text{k}\Omega$ (curve i) to $53.8\ \text{k}\Omega$ (curve ii). Since, the QCdSe-LB/ITO electrode of the chip carries positive charge, owing to the ammonium group of TOPO capping agent, and the redox marker $[\text{Fe}(\text{CN})_6]^{3-/4-}$ ions are negatively charged, the repulsion is not experienced by the $[\text{Fe}(\text{CN})_6]^{3-/4-}$ ions from the electrode surface and thus, the R_{ct} value of the chip is found to be low. However, after probe DNA immobilization, the observed significant enhancement in R_{ct} value may be correlated to the perturbation of the interfacial electron-transfer rate across the chip/electrolyte interface due to accumulation of the negative charges from phosphate ions of DNA molecules.¹¹ This enhanced negative charges at the chip surface electrostatically repels the marker $[\text{Fe}(\text{CN})_6]^{3-/4-}$ ion, resulting in an increase in R_{ct} value. All the impedance measurements have been carried out for five times and the standard deviations calculated for QCdSe-LB/ITO electrode and pDNA/QCdSe-LB/ITO electrode is found to be 0.42 and 1.24 with corresponding correlation coefficients of 0.992 and 0.987, respectively.

For DNA hybridization studies, the target DNA solution in Tris-Ethylenediaminetetraacetic acid (EDTA) buffer (TE; pH 8.0) is introduced into the microchannel through inlet and is allowed to incubate with biochip surface. The solution is discarded and the channels are washed with TE buffer to remove any non-hybridized DNA. After each experiment, $5.0\ \text{mM}$ HCl solution is passed through channels for 2 min to regenerate the sensor biochip and the regenerated biosensor yields about $<1\%$ average signal loss from each

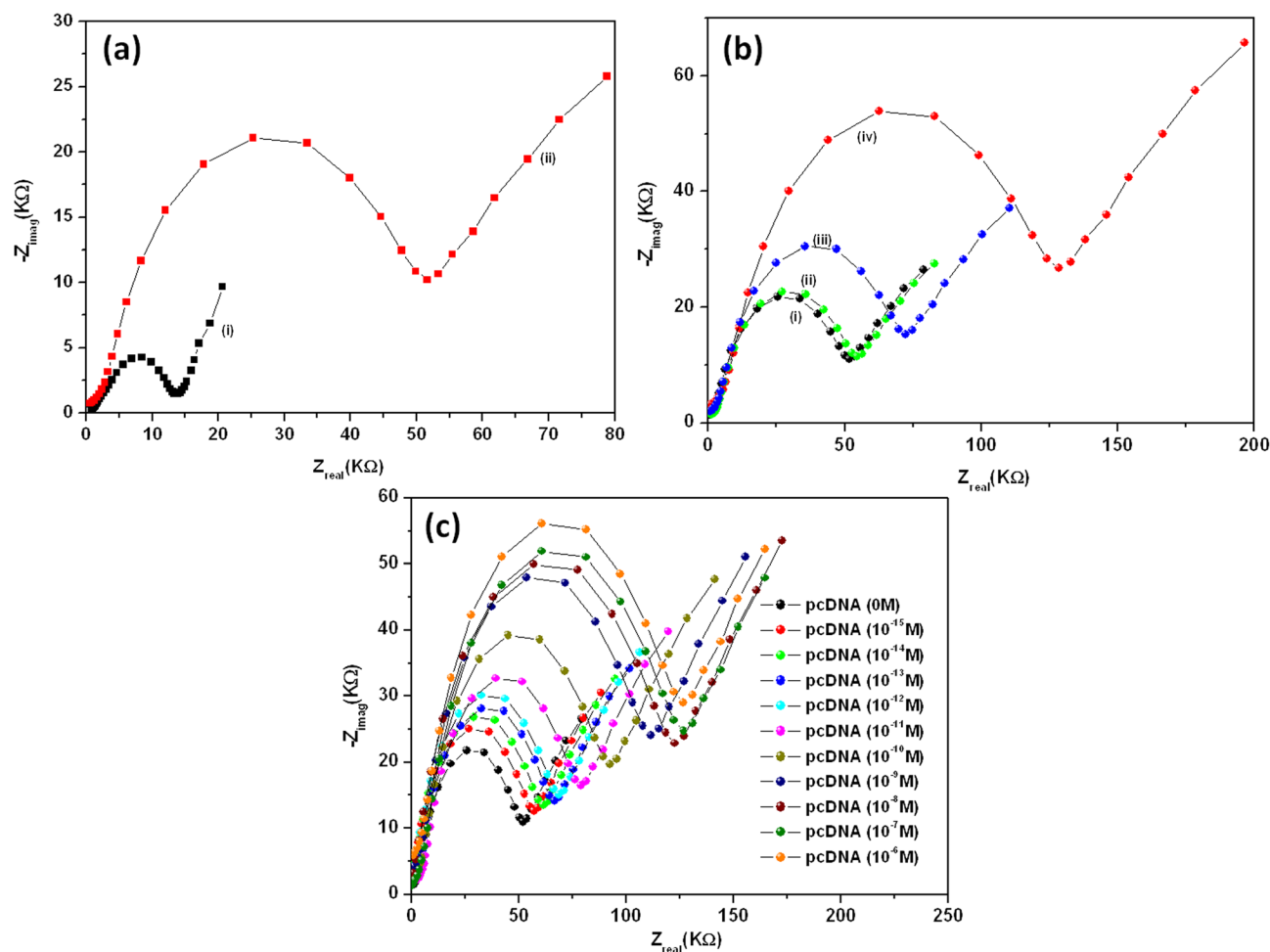


FIG. 3. (a) Nyquist diagram for the Faradic impedance of (i) chip and (ii) biochip. (b) EIS response of (i) biochip with respect to (ii) non-complementary, (iii) one-base mismatch and (iv) complementary target DNA sequence. (c) EIS responses of biochip as a function of complementary DNA concentration (10^{-15} to 10^{-6} M).

hybridization cycle (data not shown). The solution is drained and the channels are emptied followed by filling with saline (0.9% NaCl) phosphate buffer (50 mM, pH 7.0) containing 5 mM $[\text{Fe}(\text{CN})_6]^{3-/4-}$ as the redox agent.

EIS response of the microfluidic biochip towards different target DNA sequences is measured and the results are presented in Figure 3(b). Incubation with the complementary DNA results in about 2.5 fold enhancement in R_{ct} (134.5 k Ω ; curve i) of the biochip, which indicates accumulation of more negative charged moieties at biochip surface. This may further be correlated with the probe DNA hybridization with the complementary DNA strands, resulting in the double-stranded DNA helix formation that increases the negative charge of the electrode surface and consequently the R_{ct} .^{9,11,22} On incubation with the non-complementary DNA, negligible change in the R_{ct} value is observed (7.2 k Ω ; curve ii) suggesting that there is no double-stranded DNA formation occurring at the biochip surface. Since, the non-complementary DNA bases do not match the probe DNA bases, it is expected that hybridization event should not take place. The observed slight increase in R_{ct} may perhaps be due to nonspecific DNA interaction with the biochip, leading to an increased negative charge over its surface. Further, on incubation with one-base mismatch DNA sequence, there is a slight increase in the R_{ct} value

(74.4 k Ω) which is due to its hybridization with the complementary counterparts of the probe DNA (curve iii). This partial hybridization results in increased negative charge over the biochip surface due to increased blocking of the surface leading to repulsion of marker ions. These results reveal selectivity of the fabricated biochip toward different synthetic DNA sequences.

The sensitivity of the microfluidic biochip is tested with various concentrations of complementary target DNA (Figure 3(c)). The R_{ct} is found to increase with increasing complementary DNA concentration, which is due to charge accumulation by the complementary DNA, hybridized with the probe DNA strands.¹¹ This dynamic increase in R_{ct} value is observed in ten-decade concentration range from 1.0 μM to 1 fM. However, a linear variation R_{ct} with the logarithmic value of the complementary DNA concentration is obtained in the range from 10^{-15} M to 10^{-11} M (Figure S4)²³ and is presented in Eq. (1) having linear regression coefficient of 0.9935.

$$R_{ct}[\text{biochip}](k\Omega) = 1.12 (k\Omega) + 4.27 (k\Omega) [\log \times (\text{complementary DNA concentration})]. \quad (1)$$

From the above equation, it can be inferred that the linear range of the fabricated MF biochip is very much improved

and the sensitivity of the biochip is an order of magnitude higher than that of reported biosensors for cancer detection (Table ST1).²³ This increase in sensitivity is attributed to the integration and well-defined ordered organization of the quantum dots on MF electrode that provides high surface area for the immobilization of probe DNA. This microfluidic chip shows a detection capability of CML specific oligonucleotide sequences in femto-molar range, which is improved detection limit when compared to other DNA based reported biosensors for CML (Table ST1).²³

To determine the reproducibility of the proposed biosensor, coefficient of variations (CV) are calculated using the ratio of the standard deviation σ to the mean μ ($CV = \sigma/\mu$).⁹ To determine CV, two different concentrations of the complementary target DNA (10^{-15} M and 10^{-8} M) have been used. In our experiment, the CV was calculated by detecting each sample for three times for five different prepared biochips and was found to be 3.4% ($\sigma = 1.73$ and $\mu = 50.4$) and 4.8% ($\sigma = 5.78$ and $\mu = 120.2$) for 10^{-15} M and 10^{-8} M of target DNA specific to CML, respectively. The stability of microfluidic based DNA sensor was also studied, and it was found that it retains 90% of its original R_{ct} response after 30 days of storage in 100 mM phosphate buffer saline (PBS) at 4 °C (Figure S5).²³

In conclusion, a highly sensitive, selective, and reproducible microfluidic DNA biochip based on QCdSe assembled Langmuir–Blodgett film is fabricated for CML detection. Improved loading of DNA probe due to use of QCdSe in microfluidic assembly results in increased linear range and sensitivity of the device. The fabricated impedimetric biochip is self-contained, easy-to-operate, and can be utilized for POC applications. It should be interesting to utilize this microfluidic probe modified QCdSe assembled Langmuir–Blodgett electrode for detection of blood cancer in clinical samples. And this QCdSe integrated microfluidic biochip should be useful for electrochemical detection of other bioanalytes in biological fluids (e.g., antigens/antibodies).

A.S. and C.M.P. are thankful to CSIR, India, for the award of Research Fellowships. We thank Professor A. K.

Mulchandani for providing the microfluidic channels, Dr. Gajjala Sumana (CSIR–NPL, India) for useful discussions related to the microchip fabrication, and Dr. Gajender Saini (JNU, India) for conducting HRTEM experiments. We thank Department of Science and Technology for providing the facilities to carry out the work.

- ¹J. Wang, *Biosens. Bioelectron.* **21**, 1887 (2006).
- ²S. Choi, M. Goryll, L. Sin, P. Wong, and J. Chae, *Microfluid. Nanofluid.* **10**, 231 (2011).
- ³S. Prakash, M. Pinti, and B. Bhushan, *Philos. Trans. R. Soc., A* **370**, 2269 (2012).
- ⁴J. C. McDonald and G. M. Whitesides, *Acc. Chem. Res.* **35**, 491 (2002).
- ⁵P. A. Auroux, D. Iossifidis, D. R. Reyes, and A. Manz, *Anal. Chem.* **74**, 2637 (2002).
- ⁶K. J. Odenthal and J. J. Gooding, *Analyst* **132**, 603 (2007).
- ⁷J. J. Gooding, *Electroanalysis* **14**, 1149 (2002).
- ⁸Y. Yin and X. S. Zhao, *Acc. Chem. Res.* **44**, 1172 (2011).
- ⁹H. Ben-Yoav, P. H. Dykstra, W. E. Bentley, and R. Ghodssi, *Biosens. Bioelectron.* **38**, 114 (2012).
- ¹⁰Y. J. Kim, J. E. Jones, H. Li, H. Yampara-Iquise, G. Zheng, C. A. Carson, M. Cooperstock, M. Sherman, and Q. Yu, *J. Electroanal. Chem.* **702**, 72 (2013).
- ¹¹C. M. Pandey, G. Sumana, and B. D. Malhotra, *Biomacromolecules* **12**(8), 2925 (2011).
- ¹²J.-Y. Park and S.-M. Park, *Sensors* **9**, 9513 (2009).
- ¹³C. Jianrong, M. Yuqing, H. Nongyue, W. Xiaohua, and L. Sijiao, *Biotechnol. Adv.* **22**, 505 (2004).
- ¹⁴S. Lee, J. Sung, and T. Park, *Ann. Biomed. Eng.* **40**, 1384 (2012).
- ¹⁵A. Sharma, G. Sumana, S. Sapra, and B. D. Malhotra, *Langmuir* **29**, 8753 (2013).
- ¹⁶A. Sharma, C. M. Pandey, Z. Matharu, U. Soni, S. Sapra, G. Sumana, M. K. Pandey, T. Chatterjee, and B. D. Malhotra, *Anal. Chem.* **84**, 3082 (2012).
- ¹⁷S. Srivastava, M. A. Ali, P. R. Solanki, P. M. Chavhan, M. K. Pandey, A. Mulchandani, A. Srivastava, and B. D. Malhotra, *RSC Adv.* **3**, 228 (2013).
- ¹⁸M. A. Ali, P. R. Solanki, M. K. Patel, H. Dhayani, V. V. Agrawal, R. John, and B. D. Malhotra, *Nanoscale* **5**, 2883 (2013).
- ¹⁹B.-Y. Chang and S.-M. Park, *Annu. Rev. Anal. Chem.* **3**, 207 (2010).
- ²⁰M. Moisel, M. A. F. L. de Mele, and W. D. Müller, *Adv. Eng. Mater.* **10**, B33 (2008).
- ²¹J. Bisquert and A. Compte, *J. Electroanal. Chem.* **499**, 112 (2001).
- ²²L. Santiago-Rodríguez, G. Sánchez-Pomales, and C. R. Cabrera, *Electroanalysis* **22**, 399 (2010).
- ²³See supplementary material at <http://dx.doi.org/10.1063/1.4921203> for experimental section, TOPO–CdSe synthesis, HRTEM image, buffer flow rate, and comparison table.